

## ORIGINAL SCIENTIFIC PAPER

# Characterisation and antimicrobial activity of silver nanoparticles derived from *Vascellum pratense* polysaccharide extract and sodium citrate

Predrag Petrović<sup>1</sup> | Danijela Kostić<sup>1</sup> | Anita Klaus<sup>2</sup> | Jovana Vunduk<sup>2</sup> | Miomir Nikšić<sup>2</sup> | Đorđe Veljović<sup>3</sup> | Leo van Griensven<sup>4</sup>

<sup>1</sup>Innovation Center of the Faculty of Technology and Metallurgy, University of Belgrade, Karnegijeva 4, 11070 Belgrade, Serbia

<sup>2</sup>Faculty of Agriculture, University of Belgrade, Nemanjina 6, 11080 Belgrade, Serbia

<sup>3</sup>Faculty of Technology and Metallurgy, University of Belgrade, Karnegijeva 4, 11070 Belgrade, Serbia

<sup>4</sup>Plant Research International, Wageningen University and Research, P.O. Box 16, 6700 AA Wageningen, The Netherlands

### Corresponding Author:

Predrag Petrović, Innovation Center of the Faculty of Technology and Metallurgy, University of Belgrade, Karnegijeva 4, 11070 Belgrade, Serbia

Email: ppetrovic@tmf.bg.ac.rs

### Keywords:

Silver nanoparticles, mushroom polysaccharides, zeta potential, antimicrobial activity, MRSA

### Abstract

Silver nanoparticles (AgNPs) were synthesized by "green", cheap hydrothermal method in an autoclave using sodium citrate and *Vascellum pratense* polysaccharide extract as reducing and stabilizing agents. Presence of spherical AgNPs was confirmed by UV-VIS spectrophotometry and scanning electron microscopy; particle size was determined as ~ 40 nm. Even though colloidal solution had relatively low absolute value of zeta potential (-15 mV), short term stability studies suggested a stable system, with AgNPs being stabilized by both citrate and fungal polysaccharides, as FTIR spectra confirmed. The colloidal solution showed good antimicrobial activity against both G+/G- bacteria and *Candida albicans*, including methicilin resistant *Staphylococcus aureus* (MRSA). Products containing AgNPs and fungal polysaccharides, which possess various biological activities - most important being immunostimulation - may find use in treatment of skin conditions caused by pathogens.

## 1. INTRODUCTION

Silver nanoparticles (AgNPs) have been in the focus of extensive medicinal research over several decades due to their many possible applications, such as antimicrobial agents (Sondi & Salopek-Sondi, 2004), anticancer treatment (Sabaratnam et al., 2013). They have been reported to be more potent than silver ions (McVeigh, 2011) and could

be embedded into polymer matrices providing extended functionality of different medical and healthcare products (Palza, 2015). AgNPs are especially promising agents as wound dressing components (Rajendran et al., 2018). Various methods were described over the past decades for the synthesis of silver nanoparticles (Ag NPs) with

different sizes and shapes, which involved the reduction of AgNO<sub>3</sub> with a chemical reducing agent, such as NaBH<sub>4</sub> (Liu et al., 2010), hydrazine hydrate (Kim et al., 2004), formaldehyde (Chou et al., 2005), sodium formaldehyde sulfoxylate (Khanna & Subbarao, 2003), thiosalicylic acid (Wu & Hsu, 2008) and elemental hydrogen (Bhatte et al., 2012). All these chemicals are highly reactive and pose potential environmental and biological risks. In recent years, "green chemistry" has gradually become an important field and more and more people became concerned with potential environmental problems. Utilization of nontoxic chemicals, environmentally benign solvents, and renewable materials are some of the key issues that merit important consideration in a green synthetic strategy. As biological methods are environmental-friendly and non-toxic, their scale up can become economically important (Parikh et al., 2008; Mandal, et al., 2005). The green synthesis of Ag NPs involves three main steps, that must be evaluated based on green chemistry perspectives, including (1) selection of solvent medium, (2) selection of environmentally benign reducing agent, and (3) selection of nontoxic substances for the Ag NPs stability (Raveendran & Wallen, 2006). Na-citrate is a widely used reducing agent for AgNPs synthesis (Bastus et al., 2014), although obtaining high-concentration AgNP dispersions using citrate is possible only by using additional surfactants or polymers due to the restricted colloidal stability (Mikhlin et al., 2018). The application of polysaccharides for synthesis and stabilization of metal nanoparticles has recently become an active research area (Vasquez et al., 2016). Polysaccharides represent biocompatible and biodegradable polymers and silver nanoparticles have been successfully reduced in alginate, starch and seed extract by using inexpensive, simple and „green“ hydrothermal method in the autoclave (Yang & Pan, 2012; Vigneshwaran et al., 2006; Jagtap & Bapat, 2013). Mushroom water soluble polysaccharides, mostly D-glucans, are diverse polysaccharides, commonly branched and they possess various biological activities, most notably immunomodulating, tumor-inhibitory, anti-inflammatory and antinociceptive activities (Ruthes et al., 2015). The present study was thus focused to synthesize AgNPs by a simple, efficient, ecological method without using any toxic chemicals, by a hydrothermal method, using a combination of polysaccharide extract of an edible mushroom species, *Vascellum pratense* and sodium citrate. The AgNPs were tested against several microbial strains, including pathogens involved in skin infections as well as clinical isolates.

## 2. MATERIAL AND METHODS

### 2.1. Materials

*Vascellum pratense* fruiting bodies were collected in Bor, Serbia; identification of the specimens was done by dr Boris Ivančević (Department of Mycology and Lichenology, Natural History Museum, Belgrade). AgNO<sub>3</sub> was purchased from M. P. Hemija (Bielgrade, Serbia), sodium-citrate dihydrate (W302600) from Sigma (St. Louis, MO, USA), and other chemicals/solvents were either extra pure or of analytical reagent grade. Microbial strains were from the American Type Cell Collection (ATCC). Mediums for microbial cultivation were obtained from Biolife (Milan, Italy). MiliQ water was used in all experiment.

### 2.2. Polysaccharide extract preparation

Fresh specimens of *Vascellum pratense* were lyophilized, powdered and extracted with 3.8% HCl, according to (Szwengiel & Stachowiak, 2016), with slight modification; the extraction was performed in an autoclave at 1.2 bars, 100°C for 1h. After neutralization with 5M NaOH, the mixture was centrifuged and the supernatant was filtered through a filter paper (Whatman No. 5). Two volumes of ethanol were added to the filtrate to precipitate polysaccharides. The mixture was centrifuged and its precipitate collected, reconstituted in a small amount of water and then lyophilized. The obtained crude polysaccharide extract was dissolved in water and subjected to dialysis in membrane tubes (SERVAPOR, MWCO 12-14 kDa) for 48h to remove NaCl and low molecular weight fractions. After dialysis, the partially purified polysaccharide extract solution was centrifuged, supernatant collected and lyophilised. 200 mg of partially purified water soluble polysaccharide was obtained from 10g of dry mushroom fruiting body material.

### 2.3. Silver nanoparticles synthesis

Silver nanoparticles were synthesized by a hydrothermal method described by (Yang & Pan, 2012) with some modifications. Briefly, 140mg of the extract was dissolved in 40 ml of distilled water. Then 0.034 g of AgNO<sub>3</sub> was dissolved in 7 ml of water and mixed with the extract solution. After 15 min of mixing, 3 ml of 2% w/v Na-citrate solution was added drop wise. The solution was left for 15 min under vigorous stirring followed by autoclaving at a constant temperature of 100 °C at the pressure of 1.2 bars for 5 h.

## 2.4. UV-VIS Spectroscopy

UV-VIS spectrum (190-800 nm) was collected using a UV-1800 spectrophotometer (Shimadzu, USA).

## 2.5. Dynamic light scattering (DLS) and zeta potential

Size distribution and zeta potential of nanoparticles were measured using a Malvern Nano-ZS Zetasizer (Malvern, UK).

## 2.6. ATR-FTIR analysis

Fourier-transform infrared (FTIR) spectra of the pure polysaccharide extract, sodium citrate and silver nanoparticles were recorded in the attenuated total reflectance (ATR) mode between 400 and 4000  $\text{cm}^{-1}$  using a Nicolet iS10 (Thermo Scientific, Sweden) spectrometer.

## 2.7. Field-emission scanning electron microscopy (FE-SEM)

Silver nanoparticles were morphologically characterized by MIRA 3 XMU Field Emission Scanning Electron Microscope (Tescan USA Inc., Cranberry Twp, PA, USA) after drying the colloidal suspension.

## 2.8. Antimicrobial analysis

Minimum inhibitory (MIC) and bactericidal concentrations (MBC) of the extracts were determined using the broth microdilution method (CLSI 2005, Klaus et al. 2015). Antimicrobial activity was tested against 6 microbial ATCC strains (*Staphylococcus aureus* 25923, *Enterococcus faecalis* 29212, *Proteus mirabilis* 12453, *Pseudomonas aeruginosa* 27853, *Escherichia coli* 25922, *Candida albicans* 10259) and one clinical isolate of methicillin-resistant *Staphylococcus aureus* (MRSA). The antimicrobial assay was performed in 96-well microtiter plates (Sarstedt, Germany). The microbial suspensions were set to  $10^5$  colony forming units and TTC (0.0075%) was added to bacterial suspensions as a growth indicator; 50  $\mu\text{L}$  of the suspensions were added to each well containing 50  $\mu\text{L}$  of previously prepared serial dilutions of the sample, covering the range of concentrations of 1.56-3200  $\mu\text{g mL}^{-1}$ . Positive growth control was 100  $\mu\text{L}$  of pure microbial suspension and negative control the same volume of pure media. All bacterial strains were incubated 24h at 37°C, while candida was incubated 48h at 30°C. The concentration of the sample at which

there was no visible microbial growth (absence of red color for bacterial strains and absence of visible colonies for *C. albicans*) was taken as a MIC value. MBC was determined by serial sub-cultivation of the samples taken from each well on an appropriate solid medium (Muller Hinton agar for bacterial strains and Malt agar for *C. albicans*); the lowest concentration of the sample without any visible growth after repeated incubation was considered as MBC. Amoxycillin was used as a standard for bacterial strains (0.05-50  $\mu\text{g mL}^{-1}$ ) and fluconazole for *C. albicans* (0.1-100  $\mu\text{g mL}^{-1}$ ).

## 3. RESULTS AND DISCUSSION

### 3.1. Characterisation of nanoparticles

#### 3.1.1. UV-VIS and ATR-FTIR spectroscopy

Synthesis of silver nanoparticles was confirmed by UV/VIS spectrum of the solution, which showed one, relatively narrow band in the visible part of the light spectrum peaking at 425 nm (Figure 1), a characteristic of silver nanoparticles, resulting from their surface plasmon resonance (Sastry et al., 1997). FT-IR analysis (Figure 2) was performed to get a better insight into chemical changes that occur during the synthesis and possible interactions of the citrate/extract with the AgNPs.

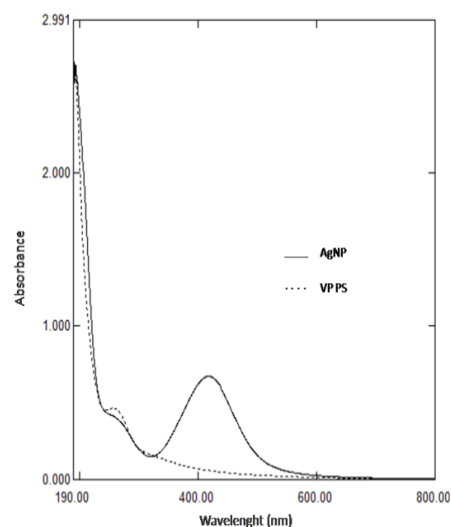


**Figure 1.** UV-VIS spectra of *V. pratense* polysaccharide extract (VP PS) and silver nanoparticle solutions (AgNP).

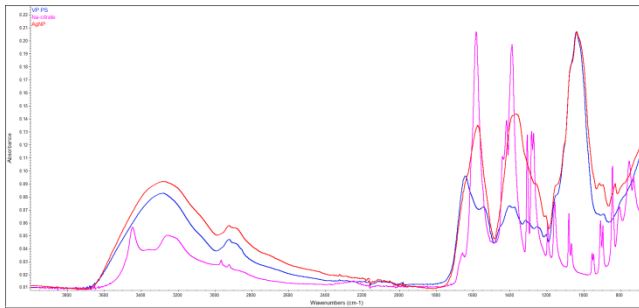


**Figure 2.** FTIR spectra of *V. pratense* polysaccharide extract (VP PS), sodium citrate (Na-citrate) and dried silver nanoparticle sample (AgNP)

FT-IR spectrum of the pure polysaccharide extract showed a broad band at  $3282\text{ cm}^{-1}$ , originating from the OH-groups (stretching vibrations), bands at  $1640$  and  $1541\text{ cm}^{-1}$  which arise from C=O bonds of the peptides, indicating presence of small amount of proteins in the extract and several overlapping bands in the region between  $1200\text{--}800\text{ cm}^{-1}$ , which come from C-O bonds, mostly of sugar monomers, with the strongest one peaking at  $1038\text{ cm}^{-1}$ . In the spectrum of sodium citrate the most pronounced are the bands of carboxylate groups, at  $1584$  and  $1387\text{ cm}^{-1}$ , which correspond to asymmetric and symmetric stretching vibrations of C=O bonds, respectively. The spectrum of air-dried AgNP colloid solution shows bands present both in the extract and citrate spectra. No definite conclusions could be made about to which degree each component (extract and citrate) takes part in the reduction of  $\text{Ag}^+$ . Bands associated with carboxylate ions, most probably coming from citrate and its degradation products (Mikhlin et al., 2018) are much broader than in the pure citrate spectra, with noticeable shoulders, suggesting that they originate from different carboxylate species and are derived from several overlapping bands. Also, peaks of these bands are shifted towards lower wavenumbers (from  $1584$  and  $1387$  to  $1574$  and  $1366\text{ cm}^{-1}$ , respectively), which may result from the weakening of C-O bonds, probably because of the interaction with AgNPs. Carboxylate groups of oxidized polysaccharide chains may also contribute to these bands' development. However, bands coming from polysaccharides kept their shape and intensity, suggesting that they mostly maintain their structure and that citrate is the main reducing agent. Peaks of the bands associated with hydroxyl groups of the sugar monomers (at  $3282\text{ cm}^{-1}$ ) and C-O sugar bonds (at  $1038\text{ cm}^{-1}$ ) also shifted to  $3269$  and  $1035\text{ cm}^{-1}$ , suggesting interaction of sugar chains with AgNPs and their additional stabilization.

### 3.1.2. Size distribution and zeta potential analysis

Size distribution by intensity analysis (Figure 3) showed that particles' size ranges from  $13.54\text{--}164.2\text{ nm}$ , with 90% of particles falling within a diameter of  $20\text{--}100\text{ nm}$  and Z-average size of  $43\text{ nm}$ .

Size distribution by intensity

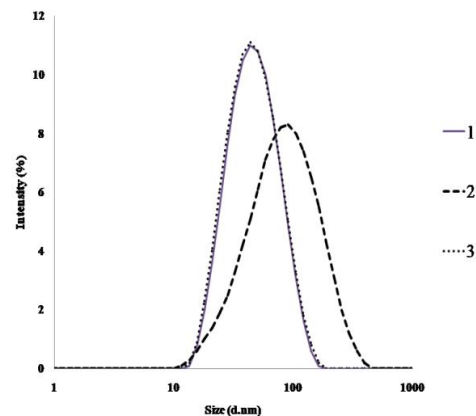


**Figure 3.** Size distribution by intensity of AgNPs on the day of synthesis (1) and three months after, without previous treatment in ultrasound bath (2) and with quick sonication (3).

The polydispersity index (PDI) of  $0.330$  also indicated a relatively uniform distribution. SEM (Figure 4) confirmed the particle size range shown by Zetasizer; particles appear to be spherical in general, but with rough surface.

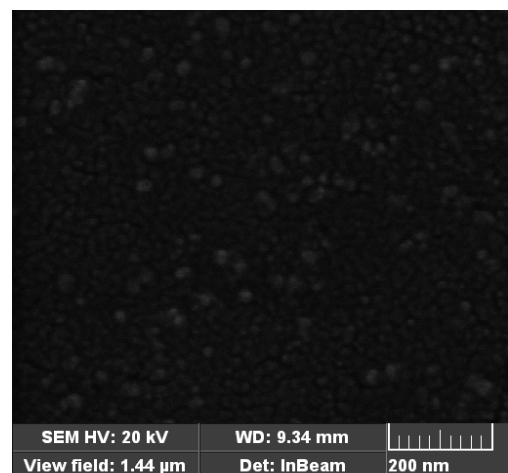


**Figure 4.** Scanning electron micrograph of silver nanoparticles

The zeta potential of pure extract solution was close to  $0$  ( $-2.7\text{ mV}$ ), which means that the polysaccharides are composed of mostly neutral

sugars; after AgNP synthesis zeta potential of the colloid dropped to -15 mV, a relatively low absolute value indicating long-term instability. However, the zeta potential did not change significantly even after 100x dilution in water, suggesting a strong relation between the silver particles and stabilizing compounds. Short-term stability analysis showed that there was a shift in size distribution of the particles towards larger diameters after 3 months at room temperature, but their aggregation was shown to be reversible after only 20s-treatment in the ultrasonic bath. Therefore, zeta potential should not be regarded as the only variable for the description of the stability of the given system, suggesting that particles are stabilized by close relationship with the polysaccharide fraction. Fungal water soluble polysaccharides, mostly glucans and mannans are branched and therefore have a great potential of steric stabilization. The dependent relationship between AgNPs and polysaccharides was shown by adding two volumes of ethanol to a AgNP solution sample, which precipitates polysaccharides; together with the polysaccharides, dark coloured AgNPs precipitated as well, leaving a pale coloured supernatant. Longer stability studies however are required for any definite conclusions.

### 3.2. Antimicrobial activity

Particles showed excellent antimicrobial activity against investigated strains (Table 1). Best activity was obtained for *P. mirabilis*, with MIC being only 12.5 µg mL<sup>-1</sup> and MBC 100 µg mL<sup>-1</sup>. Activity against other two investigated G- bacteria (*P. aeruginosa* and *E. coli*) was slightly weaker, MIC and MBC values for both strains being 100 and 200 µg mL<sup>-1</sup>, respectively. G+ bacteria (*S. aureus* and *E. faecalis*) were slightly more resistant; the growth of *S. aureus* strains, ATCC and MRSA, was inhibited at 200 µg mL<sup>-1</sup>, and bactericidal effect was achieved at 800 and 400 µg mL<sup>-1</sup>, respectively. AgNPs were least effective against *E. faecalis*, with MIC=800 µg mL<sup>-1</sup> and no bactericidal effect even at the highest concentration used. The activity against the yeast, *C. albicans* was similar, with MIC =800 µg mL<sup>-1</sup> and MBC being as high as 3.2 µg mL<sup>-1</sup>. The fungal polysaccharide extract, used as control, did not show any activity towards bacteria even at the highest concentration (20 µg mL<sup>-1</sup>) and showed only inhibitory activity against *C. albicans* at 20 µg mL<sup>-1</sup>. Antibiotics showed better activity overall, except in case of MRSA, but it should be noted that silver makes only about 17% of sample's dry mass. There seems to be a trend of slightly better activity towards G- bacteria, although differences are not significant from the clinical point of view and the

sample is too small (only 6 bacterial strains in total) studied the antimicrobial activity of AgNPs synthesized using *Ocimum gratissimum* extract, with very similar zeta potential (-15 mV) and also found better activity towards *E. coli* than *S. aureus* (that, again, was only twice as better). AgNPs synthesized by Khatoon, Nageswara Rao, Mohan, Ramanaviciene, & Ramanavicius (2017) using Na-citrate also exhibited better activity towards *E. coli* than towards G+ *B. subtilis* and had zeta-potential of around -40 mV. However, (Mandal et al., 2016) reported better activity of AgNPs towards G+ bacteria. They synthesized the particles using *Andrographis paniculata* leaf extract and tested them against multidrug resistant *Proteus vulgaris* and *Enterococcus faecalis* strains isolated from urinary tract infection (UTI) patients; they reported the zeta potential of bacteria being -26 and -15 mV, respectively and found better activity of AgNPs, which had zeta potential of -32 mV, against *E. faecalis*. The activity was only twice better in that case, too. They attributed better activity towards *E. faecalis* to the fact that tested *E. faecalis* strain had less negative zeta potential and stated that AgNPs preferentially targeted the G+ bacterium. However, in the present study *E. faecalis* turned out to be the most resistant bacterial strain and a G- bacterium, *Proteus mirabilis* the most susceptible to AgNPs, although the exact zeta potential of the tested strains was not measured. Connection between the zeta potential and antimicrobial activity of various nanoparticles was earlier reported (Arakha et al., 2015; Tamara et al., 2018), however more studies are needed to establish such a connection for silver nanoparticles. The nature of the AgNPs coating may be more important than its charge, as bacteria can recognize some types of chemical species and possibly take up AgNPs via active transport as well. Current understanding of the mechanisms of action of silver nanoparticles shows that they exhibit antimicrobial activity on several levels, disrupting the bacterial cell wall, activating reactive oxygen species once inside of cell, and being a source of Ag<sup>+</sup> ions which, like other heavy metal ions may interact with bacterial proteins and lead to their death. However, bacteria can develop mechanisms of resistance to heavy metals (Kędziora et al., 2018). Susceptibility of bacteria to silver/silver ions should be therefore regarded as a function of multiple variables and might be different not just for different species, but for different strains.

**Table 4.** Minimum inhibitory (MIC,  $\mu\text{g mL}^{-1}$ ) and bactericidal/fungicidal (MBC/MFC,  $\mu\text{g mL}^{-1}$ ) activity of silver nanoparticle colloid solution (AgNP), *V. pratense* polysaccharide extract (VP PS), amoxicillin (AMX, used only for bacterial strains) and fluconazole (FLU, used only for fungal strains), determined by the broth microdilution method.

\* Not achieved

Microbial strain	Source		AgNP	VP PS	AMX	FLU
<i>Pseudomonas aeruginosa</i>	ATCC 27853	MIC	100.00	-*	25	
		MBC	200.00		50	
<i>Proteus mirabilis</i>	ATCC 12453	MIC	12.50	-	3.25	
		MBC	100.00		12.5	
<i>Staphylococcus aureus</i>	ATCC 25923	MIC	200.00	-	0.39	
		MBC	800.00		1.56	
<i>Staphylococcus aureus</i>	clinical isolate	MIC	200.00	-	-	
		MBC	400.00		-	
<i>Escherichia coli</i>	ATCC 25922	MIC	100.00	-	6.25	
		MBC	200.00		25	
<i>Enterococcus faecalis</i>	ATCC 29212	MIC	400.00	-	0.39	
		MBC	-*		3.25	
<i>Candida albicans</i>	ATCC 10231	MIC	800.00	20		12.50
		MFC	3200.00	-		50.00

#### 4. CONCLUSION

Fungal polysaccharides are a promising agent for synthesis/stabilization of silver nanoparticles. Thanks to their branched structure, they may provide stability to the silver nano-systems with relatively low zeta-potential, which may be important as studies suggest that manipulation of zeta-potential of both AgNPs and microbial cell walls can alter antimicrobial activity. Fungal polysaccharides also exhibit other biological activities, most important being immunostimulation, so they can act synergistically with AgNPs. The AgNPs synthesized in this study showed good antimicrobial activity, of greatest clinical importance being against *P. aeruginosa*, MRSA and *C. albicans*. Preparations based on nanosilver, stabilized by biologically active fungal polysaccharides may find use in products for skin conditions caused by these pathogens.

#### ACKNOWLEDGMENT

This investigation was financially supported by the Ministry of Science and Technological Development of the Republic of Serbia, project III 46010.

#### REFERENCES

- Arakha, M., Saleem, M., Mallick, B. C., & Jha, S. (2015). The effects of interfacial potential on antimicrobial propensity of ZnO nanoparticle. *Scientific Reports*, 5(1). doi:[10.1038/srep09578](https://doi.org/10.1038/srep09578)
- Bastús, N. G., Merkoçi, F., Piella, J., & Puntès, V. (2014). Synthesis of Highly Monodisperse Citrate-Stabilized Silver Nanoparticles of up to 200 nm: Kinetic Control and Catalytic Properties. *Chemistry of Materials*, 26(9), 2836-2846. doi:[10.1021/cm500316k](https://doi.org/10.1021/cm500316k)
- Bhatte, K. D., Deshmukh, K. M., Patil, Y. P., Sawant, D. N., Fujita, S., Arai, M., & Bhanage, B. M. (2012). Synthesis of powdered silver

- nanoparticles using hydrogen in aqueous medium. *Particuology*, 10(1), 140-143.  
doi:[10.1016/j.partic.2011.05.005](https://doi.org/10.1016/j.partic.2011.05.005)
- Chou, K., Lu, Y., & Lee, H. (2005). Effect of alkaline ion on the mechanism and kinetics of chemical reduction of silver. *Materials Chemistry and Physics*, 94(2-3), 429-433.  
doi:[10.1016/j.matchemphys.2005.05.029](https://doi.org/10.1016/j.matchemphys.2005.05.029)
- CLSI (2005). Performance standards for antimicrobial susceptibility testing: 15<sup>th</sup> informational supplement. CLSI document M100-S15PA, USA: Wayne.
- Das, B., Dash, S. K., Mandal, D., Ghosh, T., Chattopadhyay, S., Tripathy, S., ... Roy, S. (2017). Green synthesized silver nanoparticles destroy multidrug resistant bacteria via reactive oxygen species mediated membrane damage. *Arabian Journal of Chemistry*, 10(6), 862-876.  
doi:[10.1016/j.arabjc.2015.08.008](https://doi.org/10.1016/j.arabjc.2015.08.008)
- Jagtap, U. B., & Bapat, V. A. (2013). Green synthesis of silver nanoparticles using *Artocarpusheterophyllus* Lam. seed extract and its antibacterial activity. *Industrial Crops and Products*, 46, 132-137.  
doi:[10.1016/j.indcrop.2013.01.019](https://doi.org/10.1016/j.indcrop.2013.01.019)
- Kędziora, A., Speruda, M., Krzyżewska, E., Rybka, J., Łukowiak, A., & Bugla-Płoskońska, G. (2018). Similarities and Differences between Silver Ions and Silver in Nanoforms as Antibacterial Agents. *International Journal of Molecular Sciences*, 19(2), 444.  
doi:[10.3390/ijms19020444](https://doi.org/10.3390/ijms19020444)
- Khanna, P., & Subbarao, V. (2003). Nanosized silver powder via reduction of silver nitrate by sodium formaldehydesulfoxylate in acidic pH medium. *Materials Letters*, 57(15), 2242-2245.  
doi:[10.1016/S0167-577X\(02\)01203-X](https://doi.org/10.1016/S0167-577X(02)01203-X)
- Khatoun, U. T., Nageswara Rao, G., Mohan, K. M., Ramanaviciene, A., & Ramanavicius, A. (2017). Antibacterial and antifungal activity of silver nanospheres synthesized by tri-sodium citrate assisted chemical approach. *Vacuum*, 146, 259-265.  
doi:[10.1016/j.vacuum.2017.10.003](https://doi.org/10.1016/j.vacuum.2017.10.003)
- Kim, K. D., Han, D. N., & Kim, H. T. (2004). Optimization of experimental conditions based on the Taguchi robust design for the formation of nano-sized silver particles by chemical reduction method. *Chemical Engineering Journal*, 104(1-3), 55-61.  
doi:[10.1016/j.cej.2004.08.003](https://doi.org/10.1016/j.cej.2004.08.003)
- Klaus, A., Kozarski, M., Vunduk, J., Todorovic, N., Jakovljevic, D., Zizak, Z., ... Van Griensven, L. J. (2015). Biological potential of extracts of the wild edible Basidiomycete mushroom *Grifolafrondosa*. *Food Research International*, 67, 272-283.  
doi:[10.1016/j.foodres.2014.11.035](https://doi.org/10.1016/j.foodres.2014.11.035)
- Liu, J., Li, X., & Zeng, X. (2010). Silver nanoparticles prepared by chemical reduction-protection method, and their application in electrically conductive silver nanopaste. *Journal of Alloys and Compounds*, 494(1-2), 84-87.  
doi:[10.1016/j.jallcom.2010.01.079](https://doi.org/10.1016/j.jallcom.2010.01.079)
- Mandal, D., Bolander, M. E., Mukhopadhyay, D., Sarkar, G., & Mukherjee, P. (2005). The use of microorganisms for the formation of metal nanoparticles and their application. *Applied Microbiology and Biotechnology*, 69(5), 485-492.  
doi:[10.1007/s00253-005-0179-3](https://doi.org/10.1007/s00253-005-0179-3)
- Mandal, D., Kumar Dash, S., Das, B., Chattopadhyay, S., Ghosh, T., Das, D., & Roy, S. (2016). Bio-fabricated silver nanoparticles preferentially targets Gram positive depending on cell surface charge. *Biomedicine & Pharmacotherapy*, 83, 548-558.  
doi:[10.1016/j.biopha.2016.07.011](https://doi.org/10.1016/j.biopha.2016.07.011)
- McVeigh, H. (2011). Topical silver for preventing wound infection. *International Journal of Evidence-Based Healthcare*, 9(4), 454-455.  
doi:[10.1111/j.1744-1609.2011.00245.x](https://doi.org/10.1111/j.1744-1609.2011.00245.x)
- Mikhlin, Y. L., Vorobyev, S. A., Saikova, S. V., Vishnyakova, E. A., Romanchenko, A. S., Zharkov, S. M., & Larichev, Y. V. (2018). On the nature of citrate-derived surface species on Ag nanoparticles: Insights from X-ray photoelectron spectroscopy. *Applied Surface Science*, 427, 687-694.  
doi:[10.1016/j.apsusc.2017.09.026](https://doi.org/10.1016/j.apsusc.2017.09.026)
- Palza, H. (2015). Antimicrobial Polymers with Metal Nanoparticles. *International Journal of Molecular Sciences*, 16(1), 2099-2116.  
doi:[10.3390/ijms16012099](https://doi.org/10.3390/ijms16012099)
- Parikh, R. Y., Singh, S., Prasad, B. L., Patole, M. S., Sastry, M., & Shouche, Y. S. (2008). Extracellular Synthesis of Crystalline Silver Nanoparticles and Molecular Evidence of Silver Resistance from *Morganellasp.*: Towards Understanding Biochemical Synthesis Mechanism. *ChemBioChem*, 9(9), 1415-1422.  
doi:[10.1002/cbic.200700592](https://doi.org/10.1002/cbic.200700592)
- Rajendran, N. K., Kumar, S. S., Houreld, N. N., & Abrahamse, H. (2018). A review on nanoparticle based treatment for wound healing. *Journal of Drug Delivery Science and Technology*, 44, 421-430.  
doi:[10.1016/j.jddst.2018.01.009](https://doi.org/10.1016/j.jddst.2018.01.009)
- Raveendran, P., Fu, J., & Wallen, S. L. (2006). A simple and "green" method for the synthesis of

- Au, Ag, and Au–Ag alloy nanoparticles. *Green Chem*, 8(1), 34-38.  
doi:[10.1039/B512540E](https://doi.org/10.1039/B512540E)
- Ruthes, A. C., Smiderle, F. R., & Iacomini, M. (2015). d -Glucans from edible mushrooms: A review on the extraction, purification and chemical characterization approaches. *Carbohydrate Polymers*, 117, 753-761.  
doi:[10.1016/j.carbpol.2014.10.051](https://doi.org/10.1016/j.carbpol.2014.10.051)
- Gurunathan, S., Raman, J., Malek, S. N. A., John, P. A., & Vikineswary, S. (2013). Green synthesis of silver nanoparticles using Ganoderma neo-japonicum Imazeki: a potential cytotoxic agent against breast cancer cells. *International journal of nanomedicine*, 8, 4399.  
doi:[10.2147/IJN.S51881](https://doi.org/10.2147/IJN.S51881)
- Sastry, M., Mayya, K., & Bandyopadhyay, K. (1997). pH dependent changes in the optical properties of carboxylic acid derivatized silver colloidal particles. *Colloids and Surfaces A: Physicochemical and Engineering Aspects*, 127(1-3), 221-228.  
doi:[10.1016/S0927-7757\(97\)00087-3](https://doi.org/10.1016/S0927-7757(97)00087-3)
- Sondi, I., & Salopek-Sondi, B. (2004). Silver nanoparticles as antimicrobial agent: a case study on E. coli as a model for Gram-negative bacteria. *Journal of Colloid and Interface Science*, 275(1), 177-182.  
doi:[10.1016/j.jcis.2004.02.012](https://doi.org/10.1016/j.jcis.2004.02.012)
- Szwengiel, A., & Stachowiak, B. (2016). Deproteinization of water-soluble  $\beta$ -glucan during acid extraction from fruiting bodies of Pleurotus ostreatus mushrooms. *Carbohydrate Polymers*, 146, 310-319.  
doi:[10.1016/j.carbpol.2016.03.015](https://doi.org/10.1016/j.carbpol.2016.03.015)
- Tamara, F., Lin, C., Mi, F., & Ho, Y. (2018). Antibacterial Effects of Chitosan/Cationic Peptide Nanoparticles. *Nanomaterials*, 8(2), 88.  
doi:[10.3390/nano8020088](https://doi.org/10.3390/nano8020088)
- Vasquez, R. D., Apostol, J. G., De Leon, J. D., Mariano, J. D., Mirhan, C. M., Pangan, S. S., ... Zamora, E. T. (2016). Polysaccharide-mediated green synthesis of silver nanoparticles from *Sargassum siliquosum* J.G. Agardh: Assessment of toxicity and hepatoprotective activity. *OpenNano*, 1, 16-24.  
doi:[10.1016/j.onano.2016.03.001](https://doi.org/10.1016/j.onano.2016.03.001)
- Vigneshwaran, N., Nachane, R., Balasubramanya, R., & Varadarajan, P. (2006). A novel one-pot 'green' synthesis of stable silver nanoparticles using soluble starch. *Carbohydrate Research*, 341(12), 2012-2018.  
doi:[10.1016/j.carres.2006.04.042](https://doi.org/10.1016/j.carres.2006.04.042)
- Wu, R., & Hsu, S. L. (2008). Preparation of highly concentrated and stable suspensions of silver nanoparticles by an organic base catalyzed reduction reaction. *Materials Research Bulletin*, 43(5), 1276-1281.  
doi:[10.1016/j.materresbull.2007.05.020](https://doi.org/10.1016/j.materresbull.2007.05.020)
- Yang, J., & Pan, J. (2012). Hydrothermal synthesis of silver nanoparticles by sodium alginate and their applications in surface-enhanced Raman scattering and catalysis. *Acta Materialia*, 60(12), 4753-4758.  
doi:[10.1016/j.actamat.2012.05.037](https://doi.org/10.1016/j.actamat.2012.05.037)